Persistence of Severe Acute Respiratory Syndrome Coronavirus 2 in Aerosol Suspensions

Alyssa C. Fears, William B. Klimstra, Paul Duprex, Amy Hartman, Scott C. Weaver, Kenneth S. Plante, Divya Mirchandani, Jessica Ann Plante, Patricia V. Aguilar, Diana Fernández, Aysegul Nalca, Allison Totura, David Dyer, Brian Kearney, Matthew Lackemeyer, J. Kyle Bohannon, Reed Johnson, Robert F. Garry, Doug S. Reed,[1] Chad J. Roy[1]

We aerosolized severe acute respiratory syndrome coronavirus 2 and determined that its dynamic aerosol efficiency surpassed those of severe acute respiratory syndrome and Middle East respiratory syndrome coronaviruses. Although we performed experiments only once in each of several laboratories, our findings suggest retained infectivity and virion integrity for up to 16 hours in respirable-sized aerosols.

Severe acute respiratory syndrome coronavirus (SARS-CoV) 2, is a readily transmissible zoonotic pathogen and the etiologic agent of the coronavirus disease (COVID-19) pandemic (*1*). To determine aerosol stability of the virus, we measured the dynamic (short-term) aerosol efficiencies of SARS-CoV-2 and compared its efficiency with those of SARS-CoV and Middle East respiratory syndrome coronavirus (MERS-CoV).

The Study

We analyzed these 3 viruses' dynamic aerosol efficiencies using 3 nebulizers, the Collison 3-jet (C3), Collison 6-jet (C6) (http://www.chtechusa.com), and Aerogen Solo (AS) (https://www.aerogen.com), to generate viral aerosols (Appendix, https://wwwnc.cdc.gov/EID/article/26/9/20-1806-App1.pdf). We performed comparative efficiency experiments once in each of 4 aerobiology laboratories (Tulane University, New Orleans, LA, USA; National Institutes of Health Integrated Research Facility [NIH-IRF], Fort Detrick, MD, USA; US Army Medical Institute for Infectious Diseases, Fort Detrick, MD, USA; and University of Pittsburgh, Pittsburgh, PA, USA). The aerosol size distributions produced by the generators used, in mass median aerodynamic diameter, were 1–3 μm and had a geometric heterodispersity of ≈1.2–1.4. Aerosols were generated into 16-liter primate head-only exposure chambers (MERS-CoV or SARS-CoV-2) or a 30-liter rodent chamber (SARS-CoV), where the overall flow was ≈1 (Tulane) or 0.5 (NIH-IRF, US Army Medical Research Institute of Infectious Diseases, University of Pittsburgh) air changes per minute. Use chamber and corresponding flow rates enabled us to determine the dynamic efficiencies of the virus in aerosols during a short residence time. Samples were continuously collected and integrated throughout the initiation of respective nebulizers into the chamber during aerosol generation events of 10–30 min. We calculated the dynamic aerosol efficiency or spray factor (*Fs*) as a unitless quotient of initial titer (PFU/L in liquid stock) to the resulting aerosol (PFU/L aerosol) providing a quantitative indicator for comparing airborne fitness (*2*,*3*).

We determined *Fs* for all 3 viruses after <1 min of chamber residence after aerosolization (Figure 1). When we compared both MERS-CoV and SARS-CoV to SARS-CoV-2 aerosols generated with a C3 nebulizer across 3 laboratories, we noted a small but significant improvement in *Fs* for SARS-CoV-2 but not

Author affiliations: Tulane University School of Medicine, New Orleans, Louisiana, USA (A.C. Fears, R.F. Garry, C.J. Roy): University of Pittsburgh, Pittsburgh, Pennsylvania, USA (W.B. Klimstra, P. Duprex, A. Hartman, D.S. Reed); University of Texas Medical Branch, Galveston, Texas, USA (S.C. Weaver, K.S. Plante, D. Mirchandani, J.A. Plante, P.V. Aguilar, D. Fernández); US Army Medical Research Institute of Infectious Diseases, Fort Detrick, Maryland, USA (A. Nalca, A. Totura, D. Dyer, B. Kearney); National Institute of Allergy and Infectious Diseases, National Institutes of Health, Fort Detrick, Maryland, USA (M. Lackemeyer, J.K. Bohannon, R. Johnson)

DOI: https://doi.org/10.3201/eid2609.201806

[1]These authors contributed equally to this article.

for SARS-CoV (p = 0.02) or MERS-CoV (p = 0.01). Because SARS-CoV was aerosolized into a different chamber/volume than MERS-CoV and SARS-CoV-2, we cannot rule out chamber effects for the difference in *Fs* between SARS-CoV and SARS-CoV-2. Our comparison of nebulizers showed improved *Fs* for SARS-CoV-2 with the C6 (p = 0.006) and the AS (p = 0.01) over the C3 but no difference between the C6 and AS (p = 0.46).

Further studies with SARS-CoV-2 at Tulane preliminarily assessed the long-term stability of airborne virus. We used a custom-built rotating (Goldberg) drum to provide an environment in which rotational drum speed overcomes the terminal settling velocity of the 2–3-μm particles, providing a static aerosol suspension of known volume (*4*–*6*). We timed aerosol samples from the drum at 10 min and 30 min and at 2 h, 4 h, and 16 h after initiation of rotation/suspension. The entire drum volume (10.7 L) was evacuated at each sampling interval and represented a discrete aerosol generation event. We quantified virus contents by plaque assay and quantitative reverse transcription PCR (qRT-PCR). We also conducted scanning electron microscopy on the collected aerosol samples as a complimentary qualitative assessment of virion integrity after longer-term aerosol suspension (Appendix). We measured environmental parameters but did not control them during the aerosol suspension experiments. The prevailing ambient environmental conditions were 23°C SD ± 2°C and 53% SD ± 11% relative humidity throughout the aerosol stability experiments. No ultraviolet light source was used within the cavity of the drum during suspensions. After initial generation of viral bioaerosols into the drum reached steady-state concentration, the drum was sealed and maintained as a static aerosol. We conducted all sampling time points once in this set of experiments.

We graphed plaque assay and qRT-PCR results and applied nonlinear least-squares regression analysis single-order decay with no outlier detection, resulting in a poor curve fit, which typically results from a lack of replicate samples. We detected infectious SARS-CoV-2 at all time points during the aerosol suspension stability experiment (Figure 2). A minor but constant fraction of SARS-CoV-2 maintained replication-competence at all time points (Figure 2, panel A), including when sampled after 16 h of aerosol suspension. This finding resulted in a remarkably flat decay curve when measured for infectivity and failed to provide a biologic half-life ($\kappa = 2.93 \times 10^{-6}$; $t_{1/2} = 2.36 \times 10^{5}$; $\tau = 3.40 \times 10^{5}$). The curve (Figure 2, panel B) from the results of split sample analysis as

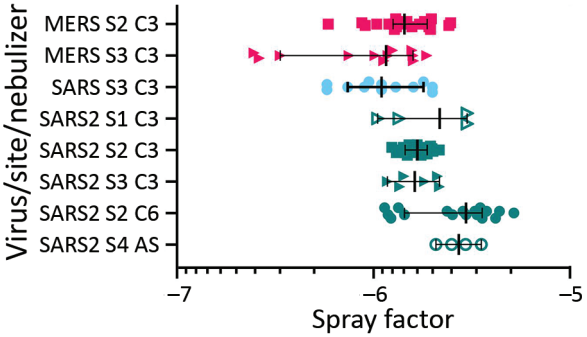

Figure 1. Aerosol efficiency of MERS-CoV, SARS-CoV and SARS-CoV-2 at different sites. Graph shows the spray factor (i.e., ratio of nebulizer concentration to aerosol concentration) for MERS-CoV (red), SARS-CoV (blue), and SARS-CoV2 (green). Aerosols were performed at 4 sites and with different nebulizers. AS, Aerogen Solo nebulizer; C3, Collison 3-jet nebulizer; C6, Collison 6-jet nebulizer; MERS-Cov, Middle East respiratory syndrome coronavirus; S1, Tulane University, New Orleans, LA, USA; S2, National Institutes of Health Integrated Research Facility, Fort Detrick, MD, USA; S3, US Army Medical Institute for Infectious Diseases, Fort Detrick, MD, USA; S4, University of Pittsburgh, Pittsburgh, PA, USA; SARS-CoV, severe acute respiratory syndrome coronavirus; SARS-CoV-2, severe acute respiratory syndrome coronavirus 2.

quantified by qRT-PCR showed minimal decreases in aerosol concentration measured in viral genome copies across all of time points sampled and approximated the decay curve of the infectious virus fraction (Figure 2, panel A), including similar decay curve characteristics ($\kappa = 6.19 \times 10^{-3}$; $t_{1/2} = 111.9$; $\tau = 161.4$).

We also performed a qualitative assessment of virion integrity after longer-term aerosol suspension (Appendix). Scanning electron microscopy (SEM) imaging of SARS-CoV-2 revealed virions that were heterogeneous in shape, either ovoid (Appendix Figure, panel A) or spherical (Appendix Figure, panel B). The minor:major axis ratio of oval virions was ≈0.7, which is consistent with prior SEM analyses of SARS-CoV-2 (https://www.flickr.com/photos/niaid/albums/72157712914621487). Airborne SARS-CoV-2 maintained the expected morphologies, size, and aspect ratios up to 16 h. Specifically, virions aged for 10 min (Appendix Figure, panels C, D) or 16 h (Appendix Figures, panels E, F) were similar in shape and general appearance to virions examined in samples of viral inoculum collected before aerosolization, which is consistent with the retention of replication-competence and suggests the potential to be infectious after long-term aging in aerosol suspension.

Conclusions

The comparison of short-term aerosol efficiencies of 3 coronaviruses showed SARS-CoV-2 approximates

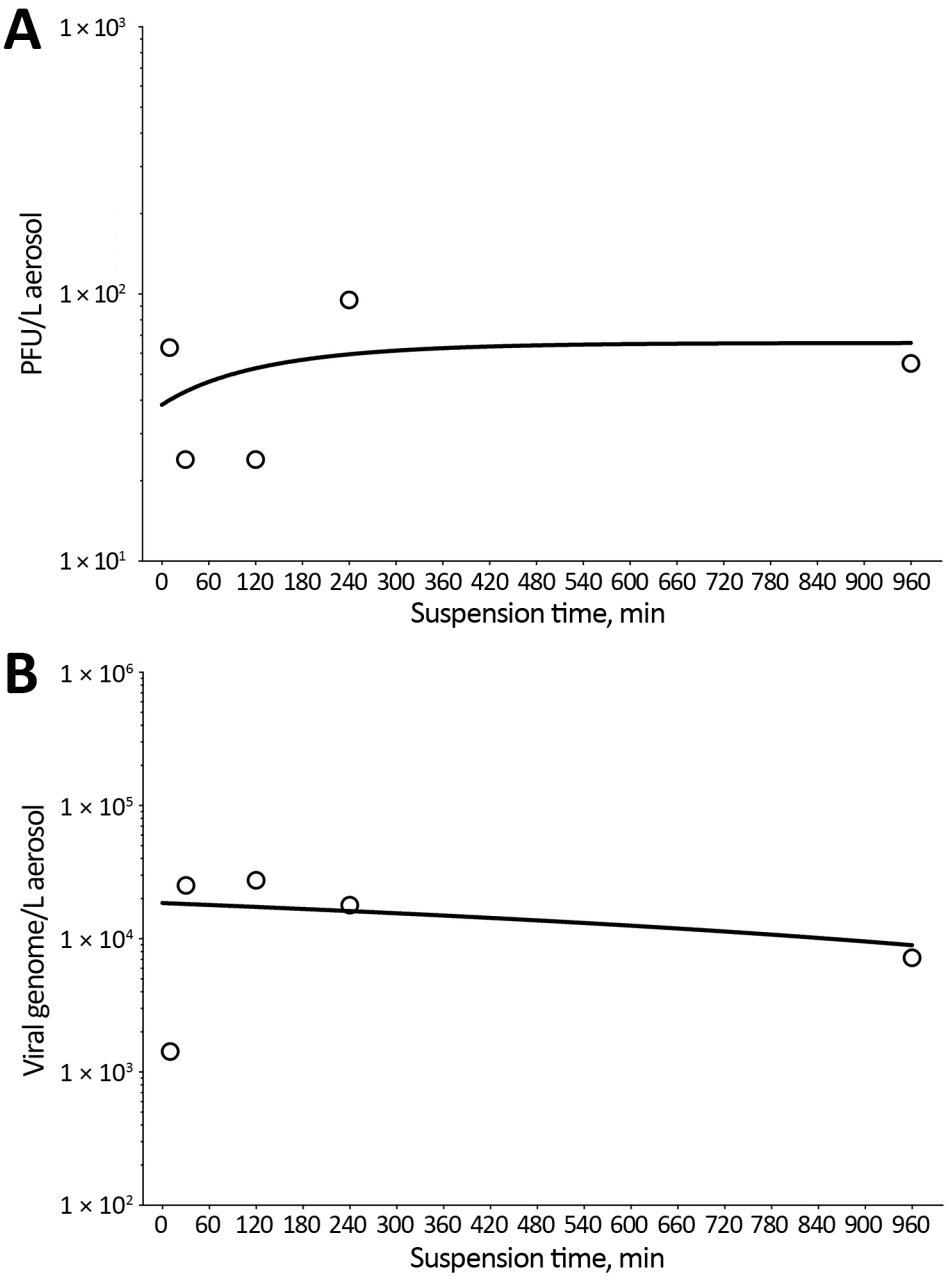

Figure 2. Decay curves of severe acute respiratory syndrome coronavirus 2 (SARS-CoV-2) in aerosol suspension. A) Aerosol concentration of infectious SARS-CoV-2 as measured by plaque assay found in impinger samples collected at 5 time points of increased aging in aerosol suspension. B) Corresponding aerosol concentration of SARS-CoV-2 in time-matched impinger samples as a function of viral genome copies as measured by reverse transcription quantitative PCR. Both time point virus estimates were graphed, and nonlinear least-squares regression analysis single-order decay with no outlier detection was performed, resulting in a poor curve fit by either method of viral quantitation resulting from number and lack of iterative samples in this analysis.

or exceeds the efficiency estimates of SARS-CoV and MERS-CoV. Some efficiency determinations for SARS-CoV-2 ranged to $-5.5^{\log 10}$ (Figure 1), a full log difference from MERS-CoV. The higher efficiencies across independent laboratories strengthens this observation. These data suggest that SARS-CoV-2 generally maintains infectivity at a respirable particle size over short distances, in contrast to either betacoronavirus. Aerosol suspension results suggest that SARS-CoV-2 persists longer than would be expected when generated as this size particle (2-μm mass median aerodynamic diameter). This finding is notable because decay and loss in the infectious fraction of airborne virus would be expected on the basis of prior susceptibility studies with other environmentally hardy viruses, such as monkeypox virus (*5*). A recent study (*6*) showing only a slight reduction of infectivity in aerosol suspensions with approximately similar particle sizes also suggested minimal effects on SARS-CoV-2 airborne degradation.

Collectively, these preliminary data suggest that SARS-CoV-2 is resilient in aerosol form, agreeing with conclusions reached in earlier studies of aerosol fitness (*6*). A limitation of our data is that we report

only 1 measurement of the 16-h time point; these findings must be replicated before definitive conclusions are reached. However, our results indicate that aerosol transmission of SARS-CoV-2 may be a more important exposure transmission pathway than previously considered (*7*). Our approach of quantitative measurement of infectivity of viral airborne efficiency augmented by assessment of virion morphology suggests that SARS-CoV-2 may be viable as an airborne pathogen. Humans produce aerosols continuously through normal respiration (*8*). Aerosol production increases during respiratory illnesses (*9*,*10*) and during louder-than-normal oration (*11*). A fraction of naturally generated aerosols falls within the size distribution used in our experimental studies (<5 μm), which leads us to conclude that SARS-CoV-2–infected persons may produce viral bioaerosols that remain infectious for long periods after production through human shedding and airborne transport. Accordingly, our study results provide a preliminary basis for broader recognition of the unique aerobiology of SARS-CoV-2, which might lead to tractable solutions and prevention interventions.

Acknowledgments

We thank Natalie Thornburg for providing 2019-nCoV/USA-WA1/2020 and Kathleen Gibson for obtaining the SARS-CoV-2 virus from the Centers for Disease Control and Prevention. We acknowledge the World Reference Center for Emerging Viruses and Arboviruses and BEI Resources, National Institute for Allergy and Infectious Diseases (NIAID), NIH, for providing MERS-CoV, EMC/2012, #NR-44260. We also thank Jenn Sword, Greg Kocher, and Dawn Gerhardt for providing all MERS-CoV and SARS-CoV-2 isolates.

This work was supported by the Intramural Research Program of the NIAID, NIH, and the Office of the Chancellor at the University of Pittsburgh. Work performed at Tulane National Primate Research Center (C.J.R., A.C.F.) was supported in part by NIH grant no. P51OD011104. R.F.G. was supported by NIH grant no. U19AI135995. Work at the University of Texas Medical Branch was supported by NIH grant no. R24AI120942. The Defense Health Program provided the funding for SARS-CoV-2 work in USAMRIID. The work at NIH-IRF was funded in part through NIAID, Division of Intramural Research and Division of Clinical Research, Battelle Memorial Institute's prime contract with NIAID under HHSN272200700016I and in whole or in part with federal funds from NIAID, NIH, US Department of Health and Human Services, HHSN272201800013C. J.K.B. performed this work as an employee of Battelle Memorial Institute. M.G.L. performed this work as an employee of Lovelace Respiratory Research Institute and Laulima Government Solutions, LLC.

About the Author

Ms. Fears is a doctoral candidate in the Biomedical Sciences Program, Department of Microbiology and Immunology, Tulane School of Medicine, Tulane University. Her primary research interests include infectious disease and immunopathogenesis of respiratory viral pathogens.

References

1. Zheng J. SARS-CoV-2: an emerging coronavirus that causes a global threat. Int J Biol Sci. 2020;16:1678–85. https://doi.org/10.7150/ijbs.45053
2. Roy CJ, Reed DS. Infectious disease aerobiology: miasma incarnate. Front Cell Infect Microbiol. 2012;2:163. https://doi.org/10.3389/fcimb.2012.00163
3. O'Malley KJ, Bowling JD, Barry EM, Hazlett KRO, Reed DS. Development, characterization, and standardization of a nose-only inhalation exposure system for exposure of rabbits to small-particle aerosols containing *Francisella tularensis*. Infect Immun. 2019;87:87. https://doi.org/10.1128/IAI.00198-19
4. Goldberg LJ, Watkins HM, Boerke EE, Chatigny MA. The use of a rotating drum for the study of aerosols over extended periods of time. Am J Hyg. 1958;68:85–93.
5. Verreault D, Killeen SZ, Redmann RK, Roy CJ. Susceptibility of monkeypox virus aerosol suspensions in a rotating chamber. J Virol Methods. 2013;187:333–7. https://doi.org/10.1016/j.jviromet.2012.10.009
6. van Doremalen N, Bushmaker T, Morris DH, Holbrook MG, Gamble A, Williamson BN, et al. Aerosol and surface stability of SARS-CoV-2 as compared with SARS-CoV-1. N Engl J Med. 2020;382:1564–7. https://doi.org/10.1056/NEJMc2004973
7. Pung R, Chiew CJ, Young BE, Chin S, Chen MI, Clapham HE, et al.; Singapore 2019 Novel Coronavirus Outbreak Research Team. Investigation of three clusters of COVID-19 in Singapore: implications for surveillance and response measures. Lancet. 2020;395:1039–46. https://doi.org/10.1016/S0140-6736(20)30528-6
8. Buonanno G, Stabile L, Morawska L. Estimation of airborne viral emission: quanta emission rate of SARS-CoV-2 for infection risk assessment. Environ Int. 2020;141:105794. https://doi.org/10.1016/j.envint.2020.105794
9. Proaño A, Bravard MA, López JW, Lee GO, Bui D, Datta S, et al.; Tuberculosis Working Group in Peru. Dynamics of cough frequency in adults undergoing treatment for pulmonary tuberculosis. Clin Infect Dis. 2017;64:1174–81. https://doi.org/10.1093/cid/cix039
10. Morawska L, Cao J. Airborne transmission of SARS-CoV-2: the world should face the reality. Environ Int. 2020;139:105730. https://doi.org/10.1016/j.envint.2020.105730
11. Stadnytskyi V, Bax CE, Bax A, Anfinrud P. The airborne lifetime of small speech droplets and their potential importance in SARS-CoV-2 transmission. Proc Natl Acad Sci U S A. 2020;117:11875–7. https://doi.org/10.1073/pnas.2006874117

Address for correspondence: Chad J. Roy, Tulane National Primate Research Center, 18703 Three Rivers Rd, Covington, LA 70433, USA; email: croy@tulane.edu

Article DOI: https://doi.org/10.3201/eid2609.201806

Persistence of Severe Acute Respiratory Syndrome Coronavirus 2 in Aerosol Suspensions

Appendix

Methods

Viruses

The viruses used for the comparative studies included SARS-CoV-2; 2019-nCoV/USA-WA1/2020 (MN985325.1), SARS-CoV-2/Munchen-1.1/2020/929; SARS-CoV, Urbani; and MERS-CoV-hNIS, and MERS-CoV Hu/Jordan-N3/2012 (KJ614529); EMC/2012 (JX869059.2). Virus stocks were prepared in Vero E6 cells and sequence confirmed by PCR and/or Sanger sequencing. Plaque assays were performed in Vero E6 cells. A manuscript is in preparation with a more detailed description of virus propagation and plaque assays (Klimstra, W., Duprex, P.).

Dynamic Aerosol Exposures

Aerosol exposures were conducted using the Automated Bioaerosol Exposure System (ABES) or AeroMP (Biaera Technologies, Hagerstown, MD, USA) exposure management platform inside a Class III biologic safety cabinet operated under negative pressure. The 3-jet (C3), 6-jet Collison (C6), or Aerogen Solo (AS) nebulizers were used for generation of aerosols. Aerosol sampling was performed with an all-glass impinger (AGI)-4 (Ace Glass, Vineland, NJ, USA) or SKC Biosampler (SKC Inc, Eighty Four, PA, USA). Aerosol particle size was determined using an Aerodynamic Particle Sizer solely or with the addition of a diluter (TSi, Shoreview, MN, USA).

SARS-CoV-2 Quantitative Real-Time Reverse Transcription PCR

Extracted nucleic acid samples were tested for SARS-CoV-2 by RT-qPCR following a previously published assay (*1*). Two RT-qPCR monoplexes targeting the N and ORF1b were used. The primers and probes used to amplify the ORF1b gene are: Forward primer [5′-TGGGGYTTTACRGGTAACCT-3′]; reverse primer [5′-AACRCGCTTAACAAAGCACTC-3′];

and probe [5′-FAM-TAGTTGTGATGCWATCATGACTAG-TAMRA-3′]. The N gene was amplified using the following primers and probe: Forward primer [5′-TAATCAGACAAGGAACTGATTA-3′]; reverse primer [5′-CGAAGGTGTGACTTCCATG-3′]; and probe [5′-FAM-GCAAATTGTGCAATTTGCGG-TAMRA-3′]. Briefly, a 20-μL reaction mixture was prepared using the iTaq Universal probes One-Step kit (BioRad, Hercules, CA, USA), according to manufacturer instructions: 10 μL of reaction mix (2×), 0.5 μL of iScript reverse transcription, 1 μL primers (10 μM), 0.5 μL probes (10 μM), 4 μL of extracted RNA and 3 μL of water. The RT-qPCR reactions were conducted using the thermocycler StepOnePlus Real-Time PCR Systems (Applied Biosystems). Reactions were incubated at 50°C for 5 min and 95°C for 20 sec followed by 40 cycles at 95°C for 5 sec and 60°C for 30 sec. Serial dilutions of the RNA extracted from a virus stock with known concentration was included for generation of a standard curve and to estimate the amount of targets in the experimental samples.

Scanning Electron Microscopy

Five mm × 2 mm hydroxyapatite (HAp) discs (Clarkson Chromatography) were incubated with 750 μL of each virus sample in DMEM media within a 24-well plate for 30 min. Sterile forceps were used to transfer each disc to 2.5% glutaraldehyde in deionized water for 12 h. Samples were further fixed in 1% osmium (VIII) oxide in 100 mM PBS for 30 min then rinsed in deionized water 3x. Samples were prepared for scanning electron microscopy by drying in successive increasing concentrations of ethyl alcohol (from 25%–100%) each for 10 min and critical point dry in a Tousimis® Autosamdri-814 dryer before mounting with carbon tape, double carbon sputter-coating in a Cressington® 208HR sputter coater, and imaging at 3 kV in a Hitachi S-3400 SEM

Analysis

Significance determined in Figure 1 by Mann-Whitney and Brown-Forsythe tests and nonlinear regression analysis in Figure 2 performed in GraphPad Prism version 8.4.1.

Reference

1. Roy CJ, Reed DS. Infectious disease aerobiology: miasma incarnate. Front Cell Infect Microbiol. 2012;2:163. PubMed https://doi.org/10.3389/fcimb.2012.00163

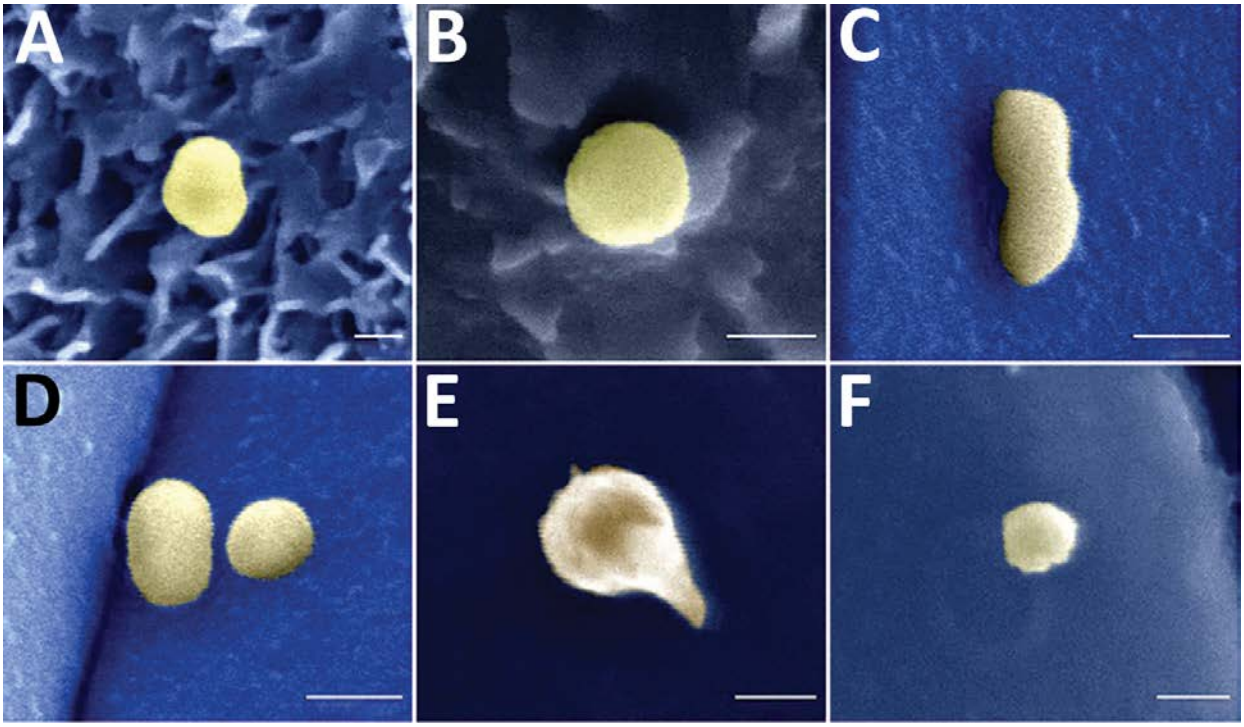

Appendix Figure. Electron microscopy images of severe acute respiratory syndrome coronavirus 2 in aerosol suspension at various timepoints. A, B) From viral stock before aerosolization. C, D) From 10-minute aerosol suspension. E, F) From 16-hour aerosol suspension. Scale bars = 100 nm.